Thermally-responsive biopolyurethanes from a biobased diisocyanate

Tamara Calvo-Correas[1], Arantzazu Santamaria-Echart[1], Ainara Saralegi[1], Loli Martin[2], Ángel Valea[3], M. Angeles Corcuera[1], Arantxa Eceiza[1]*

[1] *Group 'Materials + Technologies', Department of Chemical and Environmental Engineering, Polytechnic School, University of the Basque Country, Pza Europa 1, Donostia-San Sebastián, 20018, Spain*

[2] *Macrobehavior-Mesostructure-Nanotechnology General Research Service (SGIker) Polytechnic School, University of the Basque Country, Plaza Europa 1, 20018 Donostia-San Sebastián, Spain*

[3] *Department of Chemical and Environmental Engineering, Technical Engineering Collage of Bilbao, University o the Basque Country, Paseo Rafael Moreno "Pitxitxi" 3, 48013 Bilbao, Spain*

tamara.calvo@ehu.eus, arantzazu.santamaria@ehu.eus, ainara.saralegui@ehu.eus, loli.martin@ehu.eus, angel.valea@ehu.eus, marian.corcuera@ehu.eus
**corresponding author: arantxa.eceiza@ehu.eus*

ABSTRACT

In this work, segmented biopolyurethanes with thermally-activated shape-memory properties were synthesized and characterized. All the employed starting materials were derived from renewable sources. The macrodiol, which forms the hard segment, was derived from castor oil, while the soft segment was composed of a diisocyanate from the amino acid lysine, as well as a chain extender from corn sugar. The effect of component molar ratios and switching temperature on the shape-memory behavior was analyzed. Thermal analysis of the biopolyurethanes shows a phase separated structure. Programming at different temperatures resulted in shape-memory effects, in which shape fixation and recovery could be attributed to different phases of the physical networks. Increasing the switching temperature, shape fixity values improve, however, it has no significant effect on shape recovery values. In addition, preliminary *in vitro* cytotoxicity evaluation shows that the synthesized fully biobased biopolyurethane has a non-toxic behavior, showing its potential to be used in biomedical applications.

Key words: Biopolyurethane, biobased diisocyanate, shape-memory, temperature-memory effect

INTRODUCTION

In the last decade, the interest in the development of shape-memory polymers (SMPs) has increased considerably, finding applications in different sectors ranging from the aerospace to the biomedical (1-3). SMPs are a type of polymeric smart materials which are able to remember their original shape after being deformed, and recover it as a response to an external stimulus. Heat is one of the most common stimulus, although SMPs could be also triggered by light and moisture, among others (1,4). Generally, thermally-activated SMPs consist of two phases, the permanent phase and the thermally reversible phase. The permanent phase, obtained by physical or chemical crosslinks, is the responsible for memorizing the shape. The thermally reversible phase exhibits a phase transition temperature (T_{trans}), which can either be a glass transition (T_g) or a melting temperature (T_m), serving as a molecular switch and also enabling the fixation of the temporary shape (5-7). To study the thermally-activated shape-memory properties, the material is heated and deformed at a temperature above T_{trans}, which is named as the switching temperature (T_s), and subsequently it is quenched at a temperature below T_{trans}, in order to fix the temporary shape. When the material is reheated above T_{trans}, the original shape is restored (6).

Among thermally activated SMPs, microphase separated segmented thermoplastic polyurethanes (STPU) are noteworthy, due to the possibility of synthesizing materials with different mechanical properties and a wide range of transition temperatures, just by manipulating their composition (8). STPU are block copolymers which are usually composed by two blocks, one formed by a macrodiol (polyether or polyester diols), known as the soft segment (SS), and the other formed by a diisocyanate and a low molecular weight chain extender, known as the hard segment (HS). Microphase separation depends on block composition and length, hydrogen bonding, and crystallization extent (9-14). In thermally-activated shape-memory polyurethanes, the HS rich microphase defines the permanent shape, because it usually has a melting transition at high temperatures. Moreover, the SS rich microphase is responsible for both shape fixity and shape recovery, which happens through entropy-elastic recoiling of the amorphous phase. Moreover, in the last years, many authors are studying the so-called temperature-memory effect (TME), which occurs in materials with a broad thermal transition, meaning that the material is able to memorize the temperature at which the deformation was applied, which is within the range of the thermal transition (15-18).

Furthermore, in the last decades, the interest in the design of polyurethanes derived from renewable sources is increasing as a result of economic, environmental and social concerns (19-21). In this way, the synthesis of thermally-activated STPU based on components derived from renewable sources has been promoted in the last years (8,22,23).

In this work, besides castor oil-based macrodiol and corn sugar-based chain extender, L-lysine diisocyanate (LDI) derived from lysine amino acid was used for the synthesis of fully biobased polyurethanes. The use of LDI in the synthesis, provides, apart from the benefits mentioned before, the advantage of synthesizing polyurethanes that do not produce adverse tissue reaction and whose degradation products are considered non-toxic, as reported by Bruin et al. (24,25). Biopolyurethanes were synthesized in bulk varying the molar ratio of the components. Moreover, no chemical catalysts were used in order to avoid their potential toxicity, as there already exist data in the literature showing this handicap (26), meaning they should be removed when a biomedical application is foreseen (27). LDI is an aliphatic nonsymmetrical diisocyanate containing an ethyl ester side chain which inhibits the association by hydrogen bonding (19,33). In this way, the resultant LDI based domain, in opposite to conventional 4,4'-diphenylmethane diisocyanate (MDI) and 1,6-hexamethylene diisocyanate (HDI) diisocyanate based domains, is amorphous, and shows a low T_g. Therefore, the domain formed by LDI and chain extender, will constitute the SS, similarly to the polyurethane synthesized by M. Charlon et al. (29), and it would be the domain responsible for shape fixity. Taking into account the shape memory behavior of the material, two differentiated thermal transitions are needed. For this reason, a high molecular weight castor oil-derived macrodiol was chosen as the domain that defines the permanent shape, because it was seen in a previous work (14) that this macrodiol had a constant T_m and a melting enthalpy independent to the diisocyanate/chain extender content. To the best of our knowledge this is the first time that shape memory behavior of fully biobased polyurethanes is analyzed.

Thermal properties were measured by means of differential scanning calorimetry (DSC) and dynamic mechanical analysis (DMA) in order to establish the transition temperatures of the thermally-responsive biopolyurethanes, and to identify which of the phases was responsible for shape fixity and which for the permanent shape. The morphology of the synthesized biopolyurethanes was also analyzed by atomic force microscopy (AFM). Physicochemical, mechanical and thermally-activated shape-memory properties were analyzed using gel permeation chromatography (GPC), Fourier transform infrared spectroscopy (FTIR), performing tensile, Shore D hardness and thermo-mechanical cyclic tests. Finally, preliminary evaluation of the *in vitro* cytotoxicity and surface properties were also estimated.

EXPERIMENTAL

Materials

The macrodiol used was the poly(butylene sebacate)diol derived from castor oil, with a hydroxyl index of 32.01 mg KOH/g, determined by titration based on ASTM D 4274-88 Test Method A standard, and a number-average molecular weight of 3505 g mol^{-1} (CO3), which was characterized in a previous work (14). This macrodiol contains a 70% of renewable carbon determined by ASTM-D6866 standard procedure. Ethyl ester L-lysine diisocyanate (LDI) (226 g mol^{-1}) and corn sugar based 1,3-propanediol (PD) (76 g mol^{-1}) chain extender were supplied by CHEMOS GmBH and Quimidroga S.A., respectively. Prior to their use, the CO3 and the PD were dried under vacuum for 6 h at 80 and 40 °C, respectively. The chemical structures of the macrodiol, diisocyanate and chain extender are shown in Figure 1.

a)

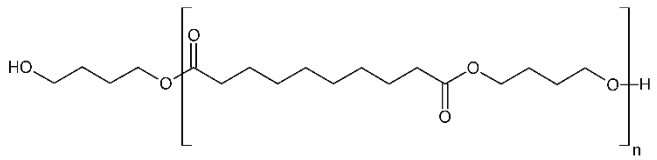

b)

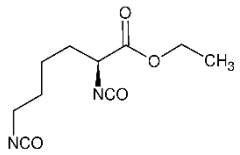

c)

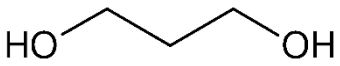

Figure 1. Structure of the different materials used in STPU synthesis: poly(butylene sebacate)diol (a), ethyl ester L-lysine diisocyanate (b) and 1,3-propanediol (c).

Synthesis of the biopolyurethanes

Biopolyurethanes were synthesized using a two-step bulk polymerization procedure. The reaction was carried out in a 250 mL five-necked round-bottom flask equipped with a mechanical stirrer and a dry nitrogen inlet. Firstly, the dried polyol and diisocyanate were placed in the flask and heated in a thermo-regulated silicon bath at 100 °C for 5 h. Then, the dry chain extender was added to the prepolymer at 100 °C while stirring vigorously for 10-15 min to homogenize the mixture. Finally, the resulting viscous liquid was quickly poured between two Teflon® coated metal plates separated by 1.5 mm and pressed at 100 °C under 50 bar for 10 h. The NCO to OH group molar ratio of all biopolyurethanes was kept constant at 1.01. Designation, CO3/LDI/PD molar ratios and LDI/PD content of the biopolyurethanes are shown in Table 1. As a reference, pure LDI/PD (PUPD100) was also synthesized.

Table 1. Designation, molar ratio, LDI/PD content, weight and number average molecular weight and polydispersity index of the biopolyurethanes.

Sample designation	CO3/LDI/PD molar ratio	LDI/PD (wt%)[a]	$\bar{M}_w$ (g mol^{-1})	$\bar{M}_n$ (g mol^{-1})	PI
PUPD13	1/2/1	13	190000	95000	2.0
PUPD19	1/3/2	19	150000	76000	2.0
PUPD29	1/5/4	29	100000	40000	2.5
PUPD40	1/8/7	40	101000	33000	3.2
PUPD50	1/12/11	50	87000	22000	3.9

[a] LDI/PD content calculated as weight percentage of LDI and PD respect to total biopolyurethane weight.

Characterization techniques

Gel permeation chromatography

Weight average and number average molecular weights, $\bar{M}_w$ and $\bar{M}_n$, respectively, and polydispersity index (PI) of the synthesized biopolyurethanes were determined by gel permeation chromatography using a Thermo Scientific chromatograph, equipped with an isocratic Dionex UltiMate 3000 pump and a RefractoMax 521 refractive index detector. The separation was carried out at 30 °C within four Phenogel GPC columns from Phenomenex, with 5 µm particle size and 10^5, 10^3, 100 and 50 Å porosities, respectively, located in a UltiMate 3000 Thermostated Colum Compartment. Tetrahydrofuran (THF) was used as mobile phase at a flow rate of 1 mL min^{-1}. Samples were prepared dissolving the obtained biopolyurethanes in THF at 1 wt% and filtering using nylon filters with 2 µm pore size. $\bar{M}_w$, $\bar{M}_n$ and PI were reported as weight average polystyrene standards.

Fourier transform infrared spectroscopy

Polyurethane characteristic functional groups and hydrogen-bonding formation were identified by means of Fourier transform infrared spectroscopy using a Nicolet Nexus FTIR spectrometer, equipped with a MKII Golden Gate accessory with diamond crystal at a nominal incident angle of 45° and a ZnSe lens. The spectra were obtained after 32 scans in a range from 4000 to 750 cm^{-1} with a resolution of 4 cm^{-1} in transmittance mode.

Differential scanning calorimetry

Thermal properties were investigated by DSC using a Mettler Toledo DSC822e equipment, provided with a robotic arm and an electric intracooler as refrigeration unit. Samples with a weight between 5 and 10 mg were sealed in aluminum pans and heated from -75 °C to 150 °C at a scanning rate of 20 ˚C min^{-1}, using N_2 as a purge gas (20 mL min^{-1}). The crystallization process was also followed by cooling the samples from 150 °C to -75 °C at a scanning rate of 10 ˚C min^{-1}. A second heating run was also performed, but as the results did not provide any extra information, it is not reported here. The observed inflexion point of the heat capacity change was chosen to evaluate glass transition temperature (T_g). Melting temperature (T_m) was settled as the maximum of the endothermic peak, taking the area under the peak as melting enthalpy (ΔH_m). Crystallization temperature (T_c) was taken as the minimum of the exothermic peak observed in the cooling scan, and the peak area as the crystallization enthalpy (ΔH_c). Taking into account the endothermic or exothermic enthalpy values, and based on equations (1) and (2), the relative crystallinity of the hard phase (χ_c) (relative crystallinity to the crystallinity of the neat macrodiol) were measured in the heating ($\chi_{c\ heating}$) and cooling ($\chi_{c\ cooling}$) scans (30) for each of the biopolyurethanes synthesized:

$$\chi_c = \Delta H_e/\Delta H_t \quad (1)$$

$$\Delta H_t = \Delta H_p * \omega \quad (2)$$

where ΔH_e is the experimental endothermic or exothermic enthalpy value, and ΔH_t is the theoretical value calculated by equation (2), where ΔH_p is the endothermic or exothermic enthalpy value of the corresponding neat phase, and ω is the weight enthalpy fraction of that phase.

Dynamic mechanical analysis

The dynamic mechanical behavior of the biopolyurethanes was analyzed by DMA in tensile mode on an Eplexor 100N analyzer from Gabo, using an initial strain of 0.10%. The temperature was varied from -100 to 150 °C at a scanning rate of 2 °C min^{-1} and at a fixed operation frequency of 10 Hz. Samples were cut in strips of 22 mm in length, 5 mm in width and 1.5 mm in thickness.

Atomic force microscopy

AFM was used to characterize biopolyurethanes morphology by imaging the cross-sections of the samples cut with a Leica EM FC6 cryo-ultramicrotome equipped with a diamond knife and operated at -120 °C. Images were obtained in tapping mode at room temperature with a Nanoscope IIIa scanning probe microscope (Multimode™ Digital Instruments), using an integrated force generated by cantilever/silicon probes, applying a resonance frequency of 180 kHz. The cantilever was 125 μm long, with a tip radius of 5-10 nm.

Mechanical properties and thermally-activated shape-memory behavior

Mechanical testing was carried out at room temperature using an Universal Testing Machine (MTS Insight 10) with a load cell of 10 kN and pneumatic grips. Samples were cut into dog-bone shape according to ASTM D1708-93 standard procedure. Tests were performed at a crosshead rate of 50 mm min^{-1}. Elastic modulus (E), tensile strength at break (σ) and percentage elongation at break (ε) were averaged from five test specimen data.

Shore D hardness measurements were performed at room temperature with a MD-202 DuroTECH digital hardness testing device, following ASTM D2240 standard procedure. Results were averaged from at least five values measured in several zones of the sample.

The thermally-activated shape-memory properties of the biopolyurethanes were studied in the strain-controlled mode using the MTS Insight 10 equipment. Samples were cut in strips of 22 mm in length, 5 mm in width and 1.5 mm in thickness, and heated at the switching temperature for 10 min. Thereafter, samples were stretched up to 50%, regardless of their initial length, at a rate of 5 mm min^{-1}. Once the goal elongation was reached, samples were cooled down below T_{trans} to fix the temporary shape, and the applied stress was removed. The permanent shape was recovered upon heating the samples up to the switching temperature for 10 min. In order to analyze the TME two different T_s were investigated. Five thermo-mechanical cyclic tensile tests were consecutively performed.

Thermally activated shape-memory behavior was quantified taking into account the commonly used parameters, i.e. shape fixity and shape recovery values. The shape fixity (R_f) and shape recovery (R_r) values can be calculated using equations 3 and 4, respectively.

$$R_f(N) = \varepsilon_u(N)/\varepsilon_m(N) \quad (3)$$

$$R_r(N) = (\varepsilon_m(N) - \varepsilon_p(N)) / (\varepsilon_m(N) - \varepsilon_p(N-1)) \quad (4)$$

where ε_m is the maximum strain in the tensile test, ε_u is the residual strain obtained after unloading the force and after cooling below T_{trans}, ε_p is the residual strain after the shape recovery, and N is the number of cycles.

Cytotoxicity

To assess *in vitro* cell response, short-term cytotoxicity evaluation was carried out using L-929 murine fibroblasts cells, following ISO 10993 recommendations (ISO 10993/EN 30993-5, 1992; ISO 10993/EN 30993-12, 1992). To prepare extracts of test materials, samples with an area of 6 cm^2 were rinsed with Mili-Q water, sterilized with 100% ethylene oxide gas, and allowed at least 7 days to degas. Sterilized film samples were incubated separately in standard cell culture medium (Dulbecco's modified Eagle's medium [Sigma Chemicals Co, USA] plus 10% fetal calf serum [Gibco] and supplemented with antibiotic-antimycotic solution [Sigma]) at 37 °C for 24 h to obtain the extracted culture media. In addition, L-929 murine fibroblasts were firstly seeded and allowed to grow in 96-well microplates at a density of 4 × 10^3 cells/well in the presence of standard culture medium for 24 h before the experiments. In the cytotoxicity test, cultures were treated for 24, 48 and 72 h with the extracted media. As controls, standard culture media (control) were used, high-density polyethylene (negative control, USP Rockville, USA) and polyvinyl chloride (positive control, Portex, UK).

To evaluate cell viability and proliferation, metabolic activity of viable cells was determined using the colorimetric assay MTT (Cell Proliferation Kit I MTT, Roche). This test is based on reduction of 3-(4,5-dimethyltriazol-2yl)-2,5 diphenyltetrazolium bromide on formazan in the mitochondria of living cells. The cell number per well was proportional to the amount of formazan crystals and was determined by measuring the absorbance at 540 nm using a microplate reader (ELISA). Viability (%) was calculated from equation 5:

$$\text{Viability (\%)} = ([A]_{test} / [A]_{control}) * 100 \quad (5)$$

where $[A]_{test}$ is the absorbance of the sample cells and $[A]_{control}$ is the absorbance of the negative control cells, in this case high-density polyethylene. All assays were conducted in triplicate, and average values and their standard deviations were estimated.

Water contact angle

The surface properties of synthesized biopolyurethanes were evaluated measuring the water contact angle (WCA) in Dataphysics OCA20 equipment. Five measurements of each sample were carried out with a deionised water drop method (2 μL) at 26 °C. The surface energy between the surface of the material and water was calculated using Neumann's Equation of State (6), which is based on the equilibrium of forces at the edge of a resting drop, as proposed by Young (10).

$$\gamma_{PU} = 1/4 \ \gamma_{H_2O} (1+\cos\beta)^2 \quad (6)$$

where γ_{PU} is the surface energy of the biopolyurethane, γ_{H_2O} is the water surface tension and β is the angle between water drop and biopolyurethane surface.

RESULTS AND DISCUSSION

Polymer properties depend strongly on their molecular weight. Therefore, the average molecular weight and polydispersity index of the synthesized biopolyurethanes are shown in Table 1. Obtained $\overline{M}_w$ and $\overline{M}_n$ values indicate that the synthesis resulted in high molecular weight biopolyurethanes. It was seen that $\overline{M}_w$ and $\overline{M}_n$ decreased with the increase of LDI/PD content, due to the lower proportion of CO3 (the reagent with the higher molar mass) involved in the synthesis of the biopolyurethanes with higher LDI/PD content. In addition, the increase

observed in PI can be attributed to vitrification, which hinders chain extension (31). In any case, the variations on the molecular weight can be ascribed to segment architecture (32).

FTIR was used to analyze the characteristic bonds of the synthesized biopolyurethanes. Figure 2 shows the infrared spectra of the synthesized biopolyurethanes and also of the neat CO3 and LDI. All biopolyurethanes spectra do not show the absorption band at 2270 cm^{-1}, associated with N=C=O group stretching vibration, indicating that all the isocyanate groups have reacted during the polymerization. Moreover, a broad band centered at 3338 cm^{-1} appears, associated to N-H stretching vibration of urethane groups, becoming more intense as isocyanate content increases, due to a higher formation of urethane groups (13). In amide II region, at 1528 cm^{-1}, the band assigned to C-N stretching vibration combined with N-H out-of-plane bending appears (9). This band also becomes more intense with the increase of diisocyanate content, owing to a higher contribution of urethane groups. As can be observed in the inset, where the infrared spectra related to amide I region (1800-1600 cm^{-1}) are shown, CO3 and LDI present a peak at 1728 and 1738 cm^{-1}, respectively, attributed to the carbonyl stretching in ester groups (32). Besides, biopolyurethanes show a band around 1728 cm^{-1} which encompasses LDI and CO3 carbonyl groups. In the same way, a shoulder ascribed to the carbonyl of urethane group was seen between 1705 and 1682 cm^{-1} (31), which becomes more intense as diisocyanate content increases, due to a higher amount of urethane groups per volume unit.

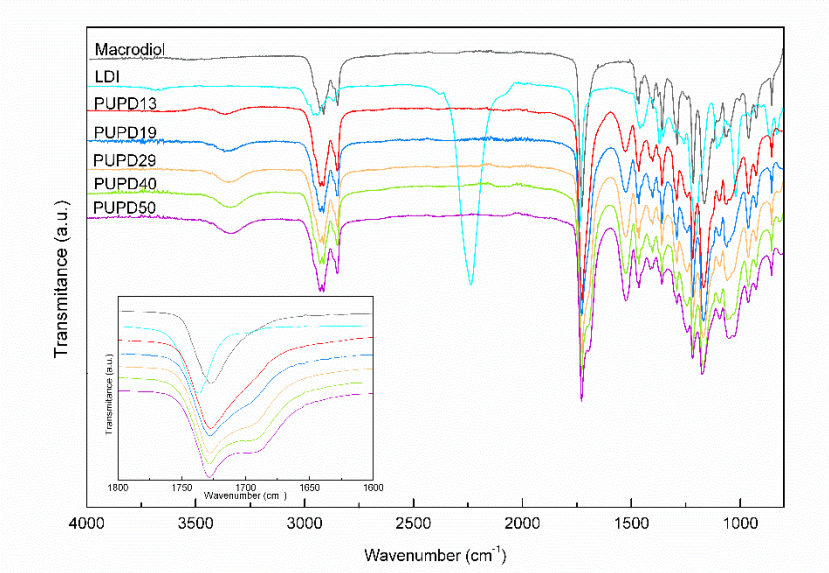

Figure 2. FTIR spectra of the synthesized biopolyurethanes, CO3 and LDI. Inset: carbonyl group stretching region.

As mentioned earlier, shape-memory polymers are formed by two phases; the thermally reversible phase, responsible for the fixity of the temporary shape, and the permanent phase, which memorizes the permanent shape (5,7). Therefore, the study of the thermal transitions and morphology of the segments has a key role to determine the test conditions, and also to understand the shape-memory behavior and the effect of T_s over this behavior. Figure 3 shows the heating DSC thermograms for the synthesized biopolyurethanes with different LDI/PD contents, together with the thermograms of CO3 and pure LDI/PD. The thermal transitions are listed in Table 2. CO3 presents a glass transition at -52 °C and an endothermic peak associated with crystals melting at 70 °C, characteristic of a semicrystalline material. Amorphous LDI/PD shows a glass transition around 33 °C. Regarding synthesized biopolyurethanes, all of them present several thermal transitions related to those observed for pure segments. Biopolyurethanes show a glass transition at low temperatures, which remains nearly constant as LDI/PD content increases. The biopolyurethanes T_g values are slightly higher than the ones

observed for CO3, indicating a microphase separation of the blocks, despite a small amount of covalently bonded LDI/PD domains could be mixed within the CO3 rich domains (9). Around 70 ºC, it can be observed an endothermic peak with a shoulder, associated with the melting temperature of an ordered microdomain mainly formed by CO3. The melting behavior depends on the distribution of crystallite sizes, the presence of different crystal forms, domain sizes and different degrees of order in the crystalline structure (9,33), and that is why the small shoulder appears. Although T_m remains nearly constant and independent of the LDI/PD content, ΔH_m decreases as LDI/PD content increases, due to the lower crystallizable CO3 fraction. As can be observed in Table 2, for the synthesized biopolyurethanes, the relative crystallinity values of the CO3 rich domain decreased respect to pure CO3 relative crystallinity values, due to covalently bonded LDI/PD domains that could inhibit the crystallization of the domain rich in CO3. Nevertheless, relative crystallinity values kept nearly constant and independent to the increase of LDI/PD content. Besides, biopolyurethanes cooling scans (Figure 3b) also show an independent behavior of crystallization temperature respect to LDI/PD content, as it remains almost at the same temperature with the increase of LDI/PD content. Although synthesized biopolyurethanes CO3 rich domain crystallization enthalpy values decrease with decreasing CO3 content, the relative crystallinity values for CO3 rich domains calculated from the exothermic peak observed in the cooling scan remains nearly constant with LDI/PD content, being similar to the one determined in the heating scan, suggesting that this phase behavior is independent of the LDI/PD content. All the biopolyurethanes show a second glass transition between the T_g and T_m of CO3 rich domain. This transition is associated with the LDI/PD domain, and increases as LDI/PD content increases, becoming closer to the value given by the neat LDI/PD, due to the formation of longer chains and showing a higher ability to join interurethane interactions (9). The low T_g value of the domain formed by LDI/PD is in agreement with the structure of LDI. For this reason, hereinafter, the domain formed by the LDI and the PD will be called as SS, and the domain rich in CO3, HS. The observation of two separated glass transitions in all biopolyurethanes suggests a microseparated phase morphology (34).

Table 2. Thermal transitions values of CO3 and the synthesized biopolyurethanes.

Sample	T_g[a] (°C)	ΔC_p[a] (J g^{-1} °C^{-1})	T_m (°C)	ΔH_m (J g^{-1})	T_g[b] (°C)		ΔC_p[b] (J g^{-1} °C^{-1})	ΔH_c (J g^{-1})	T_c (°C)	χ_c heating	χ_c cooling
CO3	-52.0	0.18	70.0	142.0	-	-	-	-93.1	46.3	1	1
PUPD13	-44.6	0.15	66.1	97.2	-8.1*	-5.0**	0.4	-58.1	36.1	0.8	0.7
PUPD19	-43.4	0.15	66.1	92.0	-0.8*	2.5**	0.4	-57.3	37.1	0.8	0.8
PUPD29	-41.8	0.15	65.4	88.3	9.2*	14.4**	0.4	-55.3	38.5	0.9	0.8
PUPD40	-	-	65.5	73.1	11.7*	19.7**	0.5	-45.5	38.9	0.9	0.8
PUPD50	-	-	66.9	57.1	12.7*	20.1**	0.4	-37.0	37.6	0.8	0.8
PUPD100	-	-	-	-	32.7*	-	0.5	-	-	-	-

[a] T_g value of the CO3-based domain measured by DSC
[b] T_g value of the LDI/PD-based domain measured by DSC (*) and DMA (**)

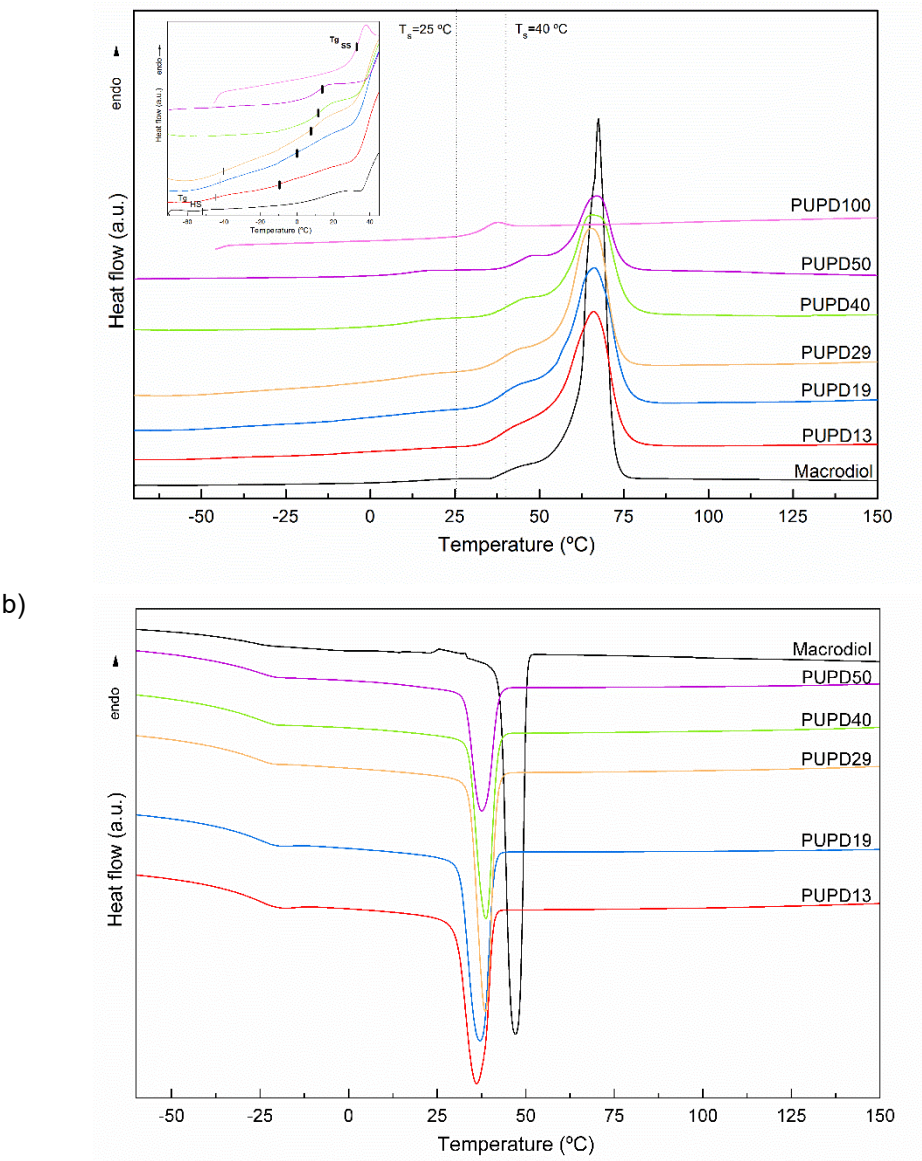

b)

Figure 3. Heating DSC thermograms of the synthesized biopolyurethanes, neat SS and CO3. Inset: magnification of low temperature region (a) and cooling DSC thermograms (b).

The dynamic mechanical behavior of the biopolyurethanes was also analyzed. The DMA technique is one of the most sensitive methods for following the changes in the viscoelastic properties. The temperature dependence of the storage modulus (E') and loss factor (tanδ) for the synthesized biopolyurethanes is shown in Figure 4. As can be seen, as SS content increases, the storage modulus (E_g) values in the glassy state increase. Therefore, one could expect that biopolyurethanes synthesized with higher SS contents would show higher R_f values, because as higher E_g values are, the greater shape fixity is (2). At lower temperatures, a broad E' decrease can be observed which encompasses both microdomains glass transition temperatures. The maximum of the peak in tanδ is related to the T_g of the SS domain. The transition temperatures are gathered in Table 2. The broadening of tanδ peak observed for PUPD13 and PUPD19 samples can be attributed to the amorphous phase of the HS. In accordance with DSC results, tanδ peak shifts to higher temperature as SS content increases. At higher temperatures, after the decrease in E' value ,the material reaches the rubbery plateau, where the rubbery modulus (E_r) value increases with the increase of HS content, due to the formation of ordered domains by semicrystalline HS, providing significant structural reinforcement and a higher elastic recovery at high temperature (2,14). Thus, biopolyurethanes

with lower SS content would show greater shape recovery values. Taking into account that a high elasticity ratio (E_g/E_r) allows an easy shaping of the material at $T > T_{trans}$ and a great resistance to the deformation at $T < T_{trans}$ (2), is expected that PUPD50 sample will present the best shape-memory properties, as can be observed in the inset of Figure 4. As PUPD13 and PUPD19 elasticity ratio values are similar, 12.4 and 11.1, respectively, the shape memory properties of PUPD13 sample were not analyzed. Finally, at higher temperatures, E' values suffer a marked decrease associated with the melting temperature of the HS, as observed also before by DSC, where a disruption of crystalline domains occurs.

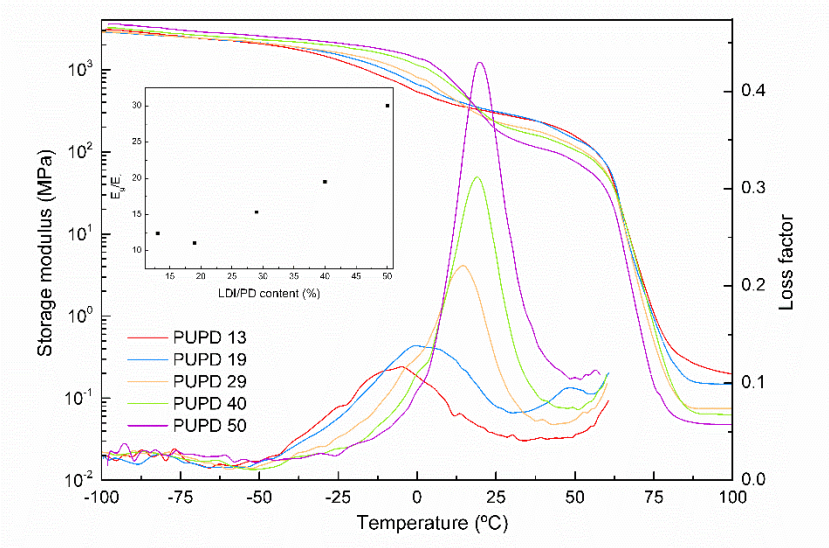

Figure 4. Storage modulus and loss factor of the synthesized biopolyurethanes. Inset: elasticity ratio (E_g/E_r) of synthesized biopolyurethanes.

Taking into account the results obtained by both DSC and DMA measurements, and after observing that the T_g of the SS domain and the T_m of the HS domain become closer as SS content increases, two switching temperatures were analyzed in order to assess shape-memory properties. Thus, the chosen temperatures were 25 and 40 ºC, which are within the interval of T_g and T_m of both domains.

The morphology of the synthesized biopolyurethanes was analyzed by AFM, and as shown in the micrographs of PUPD19 and PUPD40 (Figure 5), the synthesized biopolyurethanes present a phase separated microstructure. The light regions in height images correspond to the crystalline phase of the HS. In PUPD19 sample, almost all the surface is covered by crystalline structures, according to the high crystallinity values observed for this sample by DSC. The observed small dark regions are related to amorphous domains, which became bigger and more heterogeneous for the biopolyurethane synthesized with higher SS content. PUPD19 dark regions are ranged from 250 to 340 nm, while for PUPD40 are ranged from 370 nm to 1.5 µm.

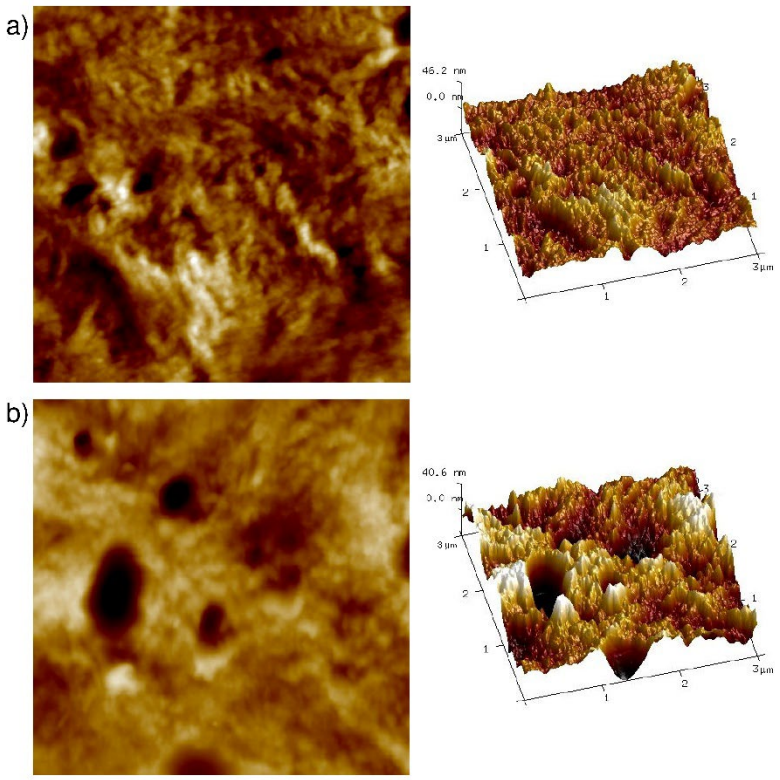

Figure 5. Height (left) and three-dimensional (right) AFM images of PUPD19 (a) and PUPD40 (b). Scan size: 3.0 x 3.0 μm^2.

Regarding mechanical behavior of the synthesized biopolyurethanes, the characteristic values derived from stress-strain curves and the Shore D hardness values are displayed in Figure 6 and Table 3. As SS content increases, the material withstands lower strains and stresses. However, the worsening of these properties is not decisive in shape-memory behavior. The increase in tensile properties observed with increasing HS content can be due to the crystallization of the HS, which acts as a reinforcing filler. As SS content increases, according to DSC results, biopolyurethane crystallinity decreases, and therefore, hardness values also decrease, as they are directly related to the overall crystallinity of the material. Taking into account the results obtained by mechanical tests, it was found that the tensile properties and hardness of the synthesized biopolyurethanes are mainly governed by HS content and crystallinity. The jumps observed in the stress-strain graphs are attributed to the formation of necking points during the tensile tests (Figure 6b), which can be due to the disruption of the crystalline domains. Thus, as HS content decreases, fewer jumps can be observed in the curves, owing to a lower amount of crystals.

Table 3. Mechanical properties of the synthesized biopolyurethane systems.

Sample	σ (MPa)	ε (%)	E (MPa)	Shore D
PUPD13	43.7 ± 3.1	1075.1 ± 52.4	223.1 ± 3.7	49.8 ± 0.8
PUPD19	28.4 ± 1.1	864.1 ± 33.4	206.4 ± 8.9	47.7 ± 0.6
PUPD29	18.5 ± 1.0	848.7 ± 31.4	142.5 ± 4.1	45.9 ± 0.5
PUPD40	14.9 ± 0.6	834.2 ± 9.9	127.5 ± 6.0	42.3 ± 0.4
PUPD50	10.6 ± 0.5	785.2 ± 18.2	89.4 ± 11.7	36.9 ± 0.3

a)

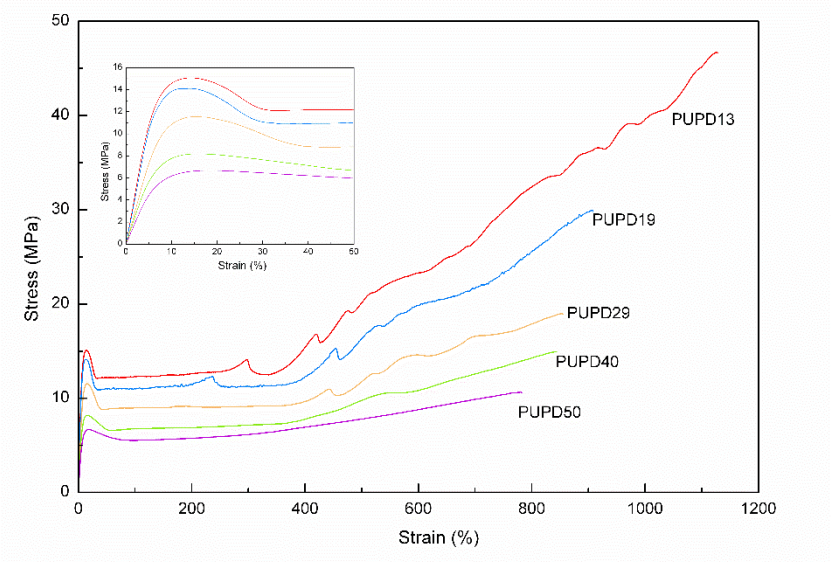

b)

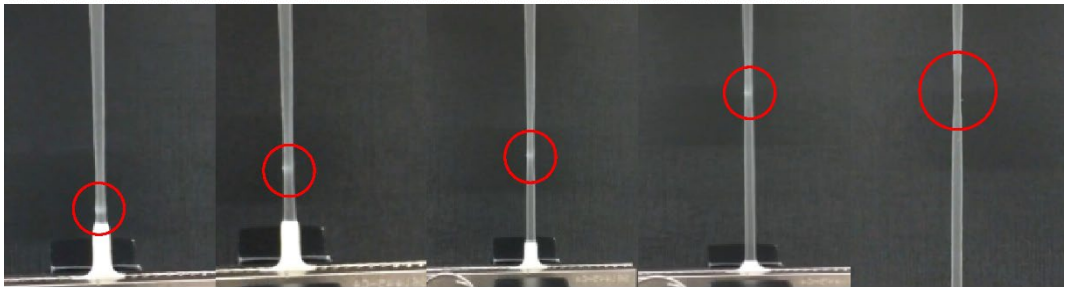

Figure 6. Stress-strain curves of the synthesized biopolyurethanes (a) and photographic sequence of the evolution of necking points during the tensile test (b).

As far as the thermally-activated shape-memory properties is concerned, the stress-strain curves for PUPD19, PUPD29, PUPD40 and PUPD50 systems thermo-mechanical cycles, taken at 25 and 40 °C, are illustrated in Figure 7. Furthermore, R_f and R_r values are summarized in Table 4. Regarding the results obtained in the first cycle at T_s = 25 ºC, R_f values of the biopolyurethanes range from 78 to 93%, and R_r values from 90 to 95%. As can be observed in Table 4, as SS content increases R_f values also increase. This could be related to the higher glass transition temperature values and higher glassy state storage modulus values observed by DMA as SS content increases.

Table 4. R_f and R_r values calculated for each thermo-mechanical cycle.

	Cycle	PUPD19		PUPD29		PUPD40		PUPD50	
		Rf	R_r	R_f	R_r	R_f	R_r	R_f	R_r
T_s = 25 °C	1	78.1	95.6	81.0	92.7	90.1	90.5	93.5	91.0
	2	78.7	99.2	81.8	98.3	91.1	98.6	91.9	99.3
	3	79.5	98.2	81.9	99.9	92.1	99.4	91.8	99.7
	4	80.3	99.6	82.3	99.7	92.2	99.8	91.8	99.7
	5	79.8	98.1	82.5	99.9	92.3	99.7	91.7	100.0
T_s = 40 °C	1	87.1	94.5	89.7	93.9	92.5	91.5	95.5	91.1
	2	86.3	98.5	89.3	99.2	92.1	99.9	94.4	98.8
	3	85.8	99.8	86.9	98.6	91.8	99.8	94.4	99.1
	4	85.8	100.0	87.1	99.6	91.8	99.8	94.4	100.0
	5	85.8	99.8	87.1	99.6	91.8	100.0	94.1	100.0

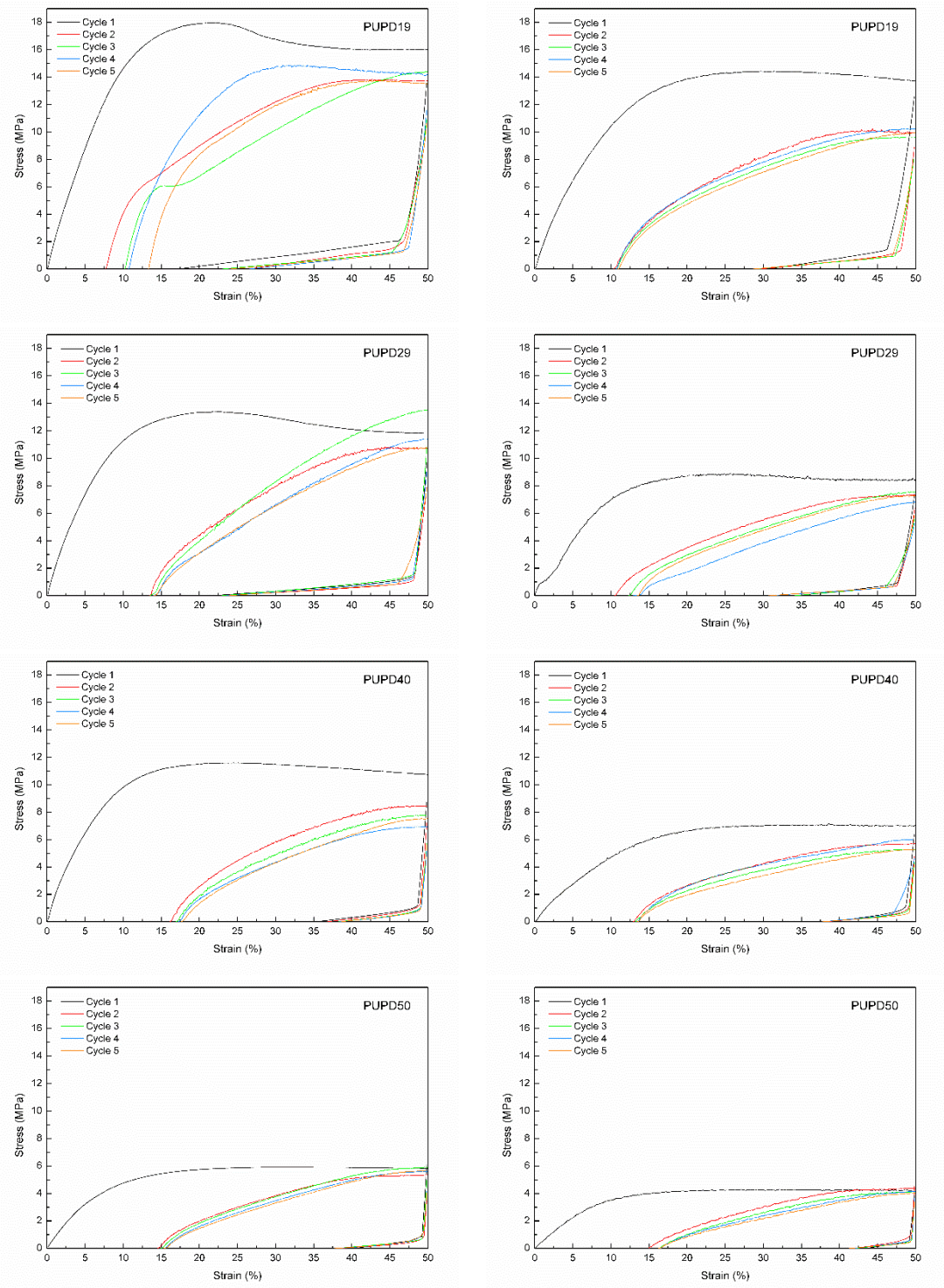

Figure 7. Stress-strain curves of thermo-mechanical cycles performed at 25 °C (left) and 40 ºC (right).

Since the original shape of thermo-responsive shape-memory polymers can be restored through crystalline structures (6), the decrease in R_r values observed when increasing the SS content of the biopolyurethanes is associated with the decrease in the amount of crystals (lower degree of crystallinity, as observed by DSC), which memorize the permanent shape. Moreover, as all samples were stretched in the first cycle over the yield point, plastic deformation occurs, resulting in the break of some interactions among crystals, which allows the shifting of the chains. Therefore, in the first cycle, the R_r values will not reach 100%, and the original shape cannot be completely restored (2,8). The residual strain left after the first thermo-mechanical

cycle increases with SS content, according to a lower crystallinity of the biopolyurethane. This means that the crystalline HS is effective acting as a fixed structure, which memorizes the original shape (6). Similar results were reported in a previous work (8), where shape fixity values were lower as crystalline domain content decreased, but in that case crystalline domains were formed by a diisocyanate and a chain extender.

Regarding thermally-activated shape-memory properties obtained for the biopolyurethanes at T_s = 40 ºC, temperature-memory effect (TME) is taking place due to the overlapping of the deformation temperature with the onset of the melting enthalpy of the HS (Figure 3a) (15,16,35). This means that the shape-memory is due to a partial thermal transition, besides of the complete ones related to the T_g of the SS domain. In this way, the HS crystals which have a T_m close to the deformation temperature, could contribute to the shape fixation. As can be seen in Table 4, and comparing the obtained R_f values for each SS composition at T_s = 25 and 40 ºC, it can be observed that R_f values increase when T_s increases. The differences between R_f values at 25 ºC and at 40 ºC for PUPD19, PUPD29, PUPD40 and PUPD50 systems are 9.4, 8.7, 2.4 and 2.0, respectively. As can be observed, the difference becomes more pronounced as HS content increases. This fact could be attributed to the melted fraction of HS crystals, contributing to the rubbery state of the polymer (15). The difference between R_f values is more marked for PUPD19 and PUPD29 samples, probably due to a higher fraction of HS, suggesting that TME depends on the HS content.

It is noteworthy that when the material is deformed at T_s = 40 °C it withstands lower stress. This could be a result of an easier disentangle of the chains as temperature increases, and also due to the higher fraction of HS in the rubbery state at this temperature. Moreover, with increasing temperature, the rubbery modulus values of polymers decrease, making the orientation more feasible (2). Similar results were found in literature for copolyesterurethanes (15), where higher shape fixity values were obtained at the highest switching temperatures. In addition, shape fixity increased as the content of the block with the highest melting temperature decreased.

The changes between the first and the remaining cycles are attributed to the history of the sample. During the first cycle, the reorganization of the polymer at molecular scale takes place, involving the redistribution in the direction of the stress (5,32). As can be seen in Figure 7, after several cycles, the thermo-mechanical properties of the material become similar, suggesting that the biopolyurethanes have stable thermo-mechanical cyclic properties, except in the case of PUPD19 at 25 °C. Analyzing the R_r values taken at 25 and 40 °C, the material recovers practically the same, despite the fact that at 40 °C some of the crystals of the HS are melted, so both temperatures are high enough to achieve the maximum shape recovery. The main difference between both temperatures is the time required to restore the shape, as at higher temperatures chain mobility increases, and it would have influence over shape recovery time. Thus, the higher the recovery temperature is, the faster the shape recovery is. Figure 8 shows real shape images of PUPD29 sample, taken along the first cycle, where different recovery times were measured at 25 and 40 °C. It can be observed that after 74 s, at 40 °C, the maximum recovery that the material was able to withstand was reached, whereas at 25 °C, the material still maintains the deformed shape. The maximum recovery at 25 °C was reached after 195 s. Once five thermo-mechanical cyclic tensile tests were performed, samples were stretched up to ε_m again, cooled down to fix the shape, and kept at 4 °C in a refrigerator. After three months, it was observed that all samples still maintained the fixed shape, and after being heated up to T_s, they restored their original shape. The obtained R_r values were similar to the ones obtained after the last cycle.

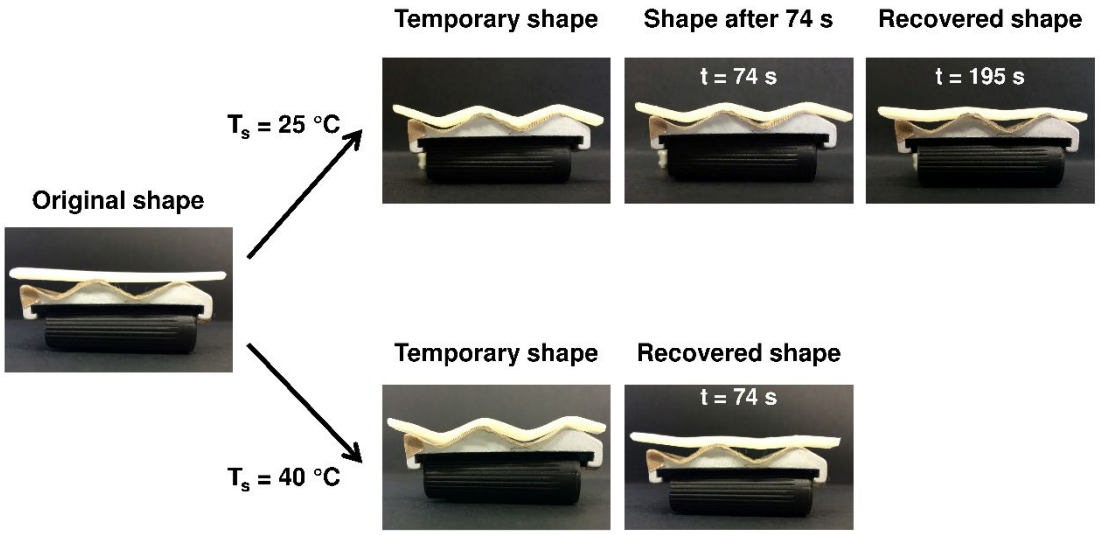

Figure 8. Real shape photographs of PUPD29, taken at the first cycle, at two different switching temperatures (T_s = 25 and 40 ºC).

Since thermally-activated shape-memory polyurethanes could be used for biomedical applications, short-term cytotoxicity assays for the synthesized biopolyurethanes were carried out. Short-term assays give information about the cell response in a sterilized material respect to the control in culture conditioned medium (36-38). Figure 9a shows the absorbance measurements determined by colorimetric assay versus incubation time for both positive (PVC) and negative (HDPE) controls, as well as for PUPD 29, and quantification of the cytotoxicity response is shown in Figure 9b. As can be observed, the synthesized biopolyurethane displayed a non-toxic behavior, close to that of the negative control. Cell viability of the sample is higher than 100% in the first 24 h, which means that the biopolyurethane results non toxic. However, after the first 24 h, the biopolyurethane presented lower cell viability, but still presents much more similarity to negative control behavior than for positive control. Moreover, ISO 10993-12 standard only takes into account the data obtained in the first 24 h.

a)

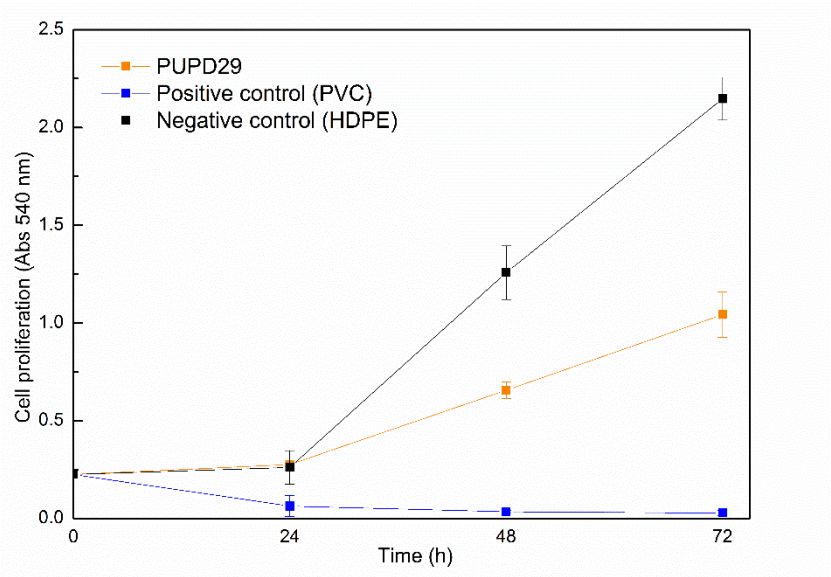

b)

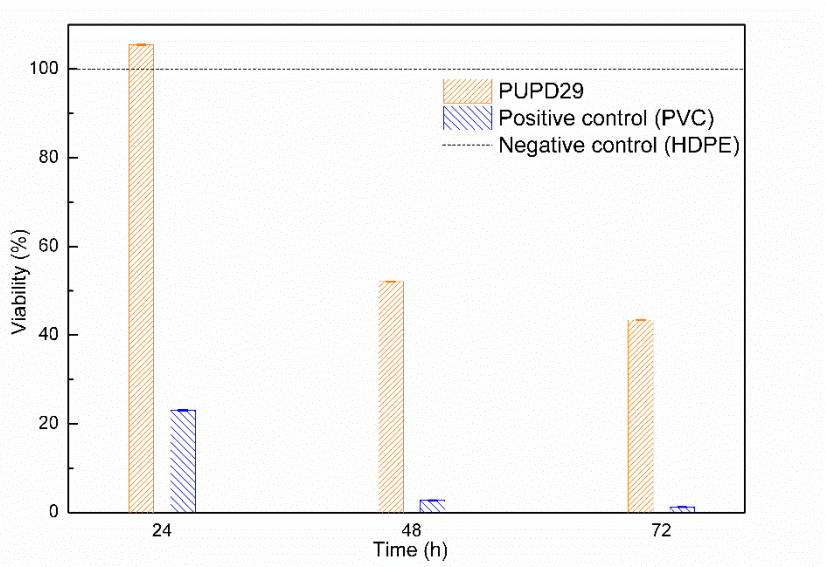

Figure 9. Absorbance at 540 nm versus incubation time of a positive control (PVC), negative control (HDPE) and PUPD29 biopolyurethane (a) and viability of L-929 murine fibroblast cells as a function of incubation time (b).

As chemical nature and domains arrangement could influence on surface properties of biopolyurethanes, such as hydrophilic character, wettability and surface tension, and therefore could deteriorate shape-memory properties, the contact angle of the synthesized biopolyurethanes was analyzed. Contact angle analysis provides information of the surface hydrophobicity or hydrophilicity, and of the molecular mobility at the air-water-solid interface (39, 40). Contact angle and surface energy values of the synthesized biopolyurethanes are given in Table 5. As SS content increases, the contact angle value decreases and surface energy increases, therefore the material becomes more hydrophilic. However, the contact angle shift is not high enough to consider a variation in thermally-activated shape-memory properties.

Table 5. Contact angle and surface energy values of synthesized biopolyurethanes.

Sample	Contact angle (°)	Surface energy (mN m^{-1})
PUPD13	81.1 ± 0.4	24.3
PUPD19	79.3 ± 0.3	25.6
PUPD29	78.4 ± 0.4	26.3
PUPD40	77.0 ± 0.2	27.3
PUPD50	74.0 ± 0.4	29.6

CONCLUSIONS

Fully biobased thermally-responsive segmented thermoplastic biopolyurethanes were synthesized consisting on a macrodiol from castor oil, a diisocyanate from L-lysine amino acid and a corn sugar based chain extender.

DSC and DMA demonstrated that the synthesized biopolyurethanes were phase separated, and that only the microdomain formed by the macrodiol was able to crystallize, which acts in this case as the HS. The microdomain formed by LDI and PD shows a low T_g and behaves as the SS. The results obtained by mechanical tests revealed that the tensile properties were governed by the macrodiol content and crystallinity. Two switching temperatures between SS glass transition and HS melting temperature were analyzed to study the thermally-activated

shape-memory properties. At the lowest switching temperature, the shape-memory behavior of biopolyurethanes showed that the shape fixity values increased as SS content increased. Regarding shape recovery values, in the first thermo-mechanical cycle, R_r values increased as HS content increased. After the first cycle, all the polyurethanes presented similar R_r values and were close to 100%, which was attributed to the erase of the thermal history. At the highest switching temperature, as a consequence of being this temperature partially overlapped with the onset of HS melting enthalpy, a TME was observed. It was seen that shape fixity values increased due to the contribution of the melted HS crystals to the rubbery state, however, it had no effect on shape recovery. In addition, biocompatibility assay demonstrated that PUPD29 exhibited no cytotoxicity. The materials synthesized in this work can be considered as smart materials.

ACKNOWLEDGEMENTS

Financial support from the Basque Government (IT-776-13) and from the Spanish Ministry of Economy and Competitiveness (MINECO) (MAT2013-43076-R) is gratefully acknowledged. We also wish to acknowledge the "Macrobehavior-Mesostructure-Nanotechnology" SGIker unit from the University of the Basque Country, for their technical support. T.C-C. thanks the University of the Basque Country for Ph.D. grant (PIF/UPV/12/200).

REFERENCES

1. J. Leng, X. Lan, Y. Liu, S. Du. *Shape-memory polymers and their composites: stimulus methods and applications*. Progress in Materials Science 2011, 56: 1077-1135
2. D. Ratna, J. Karger-Kocsis. *Recent advances in shape memory polymers and composites: a review*. Journal of Materials Science and Technology 2008, 43: 254-269
3. P.T. Mather, X. Luo, I.A. Rousseau. *Shape memory polymer research*. Annual Review of Materials Research 2009, 39: 445-471
4. G.J. Berg, M.K. McBride, C. Wang, C.N. Bowman. *New directions in the chemistry of shape memory polymers*. Polymer 2014, 55(23): 5849-5872
5. A. Lendlein, S. Kelch. Shape-memory polymers. Angewandte Chemie International Edition 2002, 41: 2034-2057
6. H.M. Jeong, J.H. Song, K.W. Chi, I. Kim, K.T. Kim. *Shape memory effect of poly(methylene-1,3-cyclopentane) and its copolymer with polyethylene*. Polymer International, 2002, 51: 275-280
7. J.L. Hu, F.L. Ji, Y.W. Wong. *Dependency of the shape memory properties of a polyurethane upon thermomechanical cyclic conditions*. Polymer International, 2005 54: 600-605
8. A. Saralegi, E.J. Foster, C. Weder, A. Eceiza, M.A. Corcuera. *Thermoplastic shape-memory polyurethanes based on natural oils.* Smart Materials and Structures *2014, 23: 025033 (9pp)*
9. M.A. Corcuera, L. Rueda, B. Fernández d'Arlas, A. Arbelaiz, C. Marieta, I. Mondragon, A. Eceiza. *Microstructure and properties of polyurethanes derived from castor oil*. Polymer Degradation and Stability 2010, 95: 2175-2184
10. L. Rueda-Larraz, B. Fernández d'Arlas, A. Tercjak, A. Ribes, I. Mondragon, A. Eceiza. *Synthesis and microstructure-mechanical property relationships of segmented*

polyurethanes based on a PCL-PTHF-PCL block copolymer as soft segment. European Polymer Journal 2009, 45: 2096-2109

11. C. Wang, D.J. Kenney. *Effect of hard segments on morphology and properties of thermoplastic polyurethanes*. Journal of Elastomers and Plastics 1995, 27: 183-199

12. H. Kim, T. Lee, J. Huh, D. Lee. *Preparation and properties of segmented thermoplastic polyurethane elastomers with two different soft segment*s. Journal of Applied Polymer Science 1999, 73: 345-352

13. Y.M. Tsai, T.L. Yu, Y.H. Tseng. *Physical properties of crosslinked polyurethane*. Polymer International 1998, 47: 445-450

14. A. Saralegi, L. Rueda, B. Fernández-d'Arlas, I. Mondragon, A. Eceiza, M.A. Corcuera. *Thermoplastic polyurethanes from renewable resources: effect of soft segment chemical structure and molecular weight on morphology and final properties*. Polymer International 2013, 62: 106-115

15. K. Kratz, U. Voigt, A. Lendlein. *Temperature-memory effect of copolyesterurethanes and their application potential in minimally invasive medical technologies*. Advanced Functional Materials 2012, 22: 3057-3065

16. C. Samuel, S. Barrau, J.M. Lefebvre, J.M. Raquez, P. Dubois. *Designing multiple-shape memory polymers with miscible polymer blends: evidence and origins of a triple-shape memory effect for miscible PLLA/PMMA blends*. Macromolecules 2014, 47: 6791-6803

17. U. Nöchel, C.S. Reddy, K. Wang, J. Cui, I. Zizak, M. Behl, K. Kratz and A. Lendlein. *Nanostructural changes in crystallizable controlling units determine the temperature-memory of polymers*. Journal of Materials Chemistry A 2015, 3: 8284-8293

18. K. Yu, H.J. Qi. *Temperature memory effect in amorphous shape memory polymers*. Soft Matter 2014, 14: 9423-9432

19. G. Lligadas, J.C. Ronda, M. Galià, V. Cádiz. *Plant oils as platform chemicals for polyurethane synthesis: current state-of-the-art*. Biomacromolecules 2010, 11: 2825-2835

20. L. Hojabri, X. Kong, S. Narine. *Fatty acid-derived diisocyanate and biobased polyurethane produced from vegetable oil: synthesis, polymerization, and characterization*. Biomacromolecules 2009, 10: 884-891

21. J. Datta, E. Glowinska. *Chemical modifications of natural oils and examples of their usage for polyurethane synthesis*. Journal of Elastomers and Plastics 2014, 46 (1): 33-42

22. X. Gu, P.T. Pather. *Entanglement-based shape memory polyurethanes: synthesis and characterization*. Polymer 2012, 53: 5924-5934

23. P.T. Knight, K.M. Lee, H. Qin, P.T. Mather. *Biodegradable thermoplastic polyurethanes incorporating polyhedral oligosilsesquioxane*. Biomacromolecules 2008, 9: 2458-2467

24. P. Bruin, G.J. Veenstra, A.J. Nijenhuis, A.J. Pennings. *Design and synthesis of biodegradable poly(ester-urethane) elastomer networks composed of non-toxic building blocks*. Makromoleculare Chemie-Rapid Comunications 1988, 9: 589-894

25. P. Bruin, J. Smedinga, A.J. Pennings. *Biodegradable lysine diisocyanate-based poly(glycolide-co-e-caprolactone)-urethane network in artificial skin*. Biomaterials 1990, 11: 291-295

26. M.C. Tanzi, P. Verderio, M.G. Lampugnani, M. Resnati, E. Dejana, E. Sturani. *Cytotoxicity of some catalysts commonly used in the synthesis of copolymers for biomedical use*. Journal of Material Science. Materials in Medicine 1994, 5: 393-396

27. K. Gorna, S. Gogolewski. Biodegradable porous polyurethane scaffolds for tissue repair and regeneration. Journal of Biomedical Materials Research Part A 2006, 79A (1): 128-138

28. G.A. Skarja, K.A. Woodhouse. *Structure-property relationships of degradable polyurethane elastomers containing an amino acid-based chain extender*. Journal of Applied Polymer Science 2000, 75: 1522-1534

29. M. Charlon, B. Heinrich, Y. Matter, E. Couzigné, B. Donnio, L. Avérous. *Synthesis, structure and properties of fully biobased thermoplastic polyurethanes, obtained from a diisocyanate based on modified dimer fatty acids, and different renewable diols*. European Polymer Journal 2014, 61: 197-205

30. B. Wunderlinch. Thermal analysis of polymeric materials. 2005 (Berlin: Springer)

31. L. Ugarte, B. Fernández-d'Arlas, A. Valea, M.L. González, M.A. Corcuera, A. Eceiza. *Morphology-properties relationship in high-renewable content polyurethanes*. Polymer Engineering and Science 2014, 54(10): 2282-2291

32. B. Fernández-d'Arlas, J.A. Ramos, A. Saralegi, M.A. Corcuera, I. Mondragon, A. Eceiza. *Molecular engineering of elastic and strong supertough polyurethanes*. Macromolecules 2012, 45: 3436-3443

33. E. del Rio, G. Lligadas, J.C. Ronda, M. Galià, V. Cádiz. *Biobased polyurethanes from polyether polyols obtained by ionic-coordinative polymerization of epoxidized methyl oleate*. Journal of Polymer Science: Part A: Polymer Chemistry 2010, 48: 5009-5017.

34. A. Lendlein, R. Langer. *Biodegradable, Elastic Shape-Memory Polymers for Potential Biomedical Applications*. Science 2002, 2096: 1673-1676

35. Y. Wang, J. Li, X. Li, Y. Pan,Z. Zheng, X. Ding, Y. Peng. *Relation between temperature memory effect and multiple-shape memory behaviors based on polymer networks*. Royal Society of Chemistry 2014, 4: 20364–20370

36. A. Saralegi, S.C.M. Fernandes, A. Alonso-Varona, T. Palomares, E.J. Foster, C. Weder, A. Eceiza, M.A. Corcuera. *Shape-memory bionanocomposites based on chitin nanocrystals and thermoplastic polyurethane with a highly crystalline soft segment*. Biomacromolecules 2013, 14: 4475−4482

37. L. Rueda, A. Saralegi, B. Fernández-d'Arlas, Q. Zhou, A. Alonso-Varona, L.A. Berglund, I. Mondragon, M.A. Corcuera, A. Eceiza. *In situ polymerization and characterization of elastomeric polyurethane-cellulose nanocrystal nanocomposites. Cell response evaluation*. Cellulose 2013, 20: 1819-1828

38. L. de Nardo, S. Bertoldi, A. Cigada, M.C. Tanzi, H.J. Haugen, S. Farè. *Preparation and characterization of shape memory polymer scaffolds via solvent casting/particulate leaching*. Journal of Applied Biomaterials and Functional Materials 2012, 10(2): 119-126

39. M.A. Corcuera, L. Rueda, A. Saralegui, M.D. Martín, B. Fernández-d'Arlas, I. Mondragon, A. Eceiza. *Effect of diisocyanate structure on the properties and microstructure of polyurethanes based on polyols derived from renewable resources.* Journal of Applied Polymer Science 2011, 122: 3677-3685

40. H. Yeganeh, M.M. Lakouraj, S. Jamshidi. *Synthesis and characterization of novel biodegradable epoxy-modified polyurethane elastomers*. Journal of Polymer Science: Part A: Polymer Chemistry 2005, 43: 2985-2996